A Framework for Automated Alignment & Layer Identification of X-Ray Tomography Imaged PCBs

Ulbert J. Botero, Navid Asadizanjani, Damon L. Woodard, Domenic Forte
jbot2016@ufl.edu,(nasadi, dwoodard, dforte)@ece.ufl.edu

***Abstract*—The current state-of-the-art for reverse engineering (RE) of printed circuit boards (PCBs) is achieved non-destructively via X-Ray Computed Tomography (CT). However, the PCB RE process still remains very costly in terms of manpower, time, and reliance upon Subject Matter Experts (SME). For practical RE to be possible for applications such as obsolescence mitigation and hardware assurance, it is important that this process be as automated and fast as possible. This paper addresses a key component necessary to automate the entire process by, for the first time to the best of our knowledge, introducing a framework to identify which slices of an X-Ray CT 3-D PCB stack belong to what layer on a physical PCB in an automated, generalizable, and completely unsupervised fashion. This is demonstrated on a 6 layer PCB. Additionally, an unsupervised iterative 3-D CT stack alignment algorithm is provided for pre-processing prior to layer identification. The completion of this step in the automated PCB RE process facilitates improved performance in later RE stages.**

***Keywords*—printed circuit board; reverse engineering; machine learning; clustering; computer vision; pattern recognition; X-ray computed tomography;**

[1]

I. Introduction

Reverse Engineering (RE) of electronics involves taking an integrated circuit (IC) or printed circuit board (PCB) and retrieving its design layout and/or netlist, stored information (memory, code, firmware), and functionality/specifications. Once obtained, this information can be used for a variety of dishonest or honest intentions, ranging from illegal cloning of designs to detecting Intellectual Property (IP) infringement and piracy [1]. Additionally, RE is useful for detecting a variety of other hardware attack vulnerabilities such as hardware Trojan insertion or tampering. While there are run time and test time monitoring techniques developed to assist in detecting these hardware attacks, there is none more effective and trustworthy than a full-blown RE of a device or system. Hardware trust and assurance is especially important at the PCB level where not only are modifications and altered designs difficult to detect but can have drastic application effects.

However, full-blown RE is currently a very costly, manual, and subject matter expert (SME) reliant task. Traditionally, PCB RE has been a destructive process that involves sanding, delayering, and optical imaging a PCB layer by layer [2]. When completed, the original PCB sample is no longer useable. To address this shortcoming, the most advanced RE of PCBs relies on X-ray Computed Tomography (CT) systems, which are capable of non-destructively reproducing a 3-d point cluster of the PCB sample and reconstructing the board [3]. This 3-d point cluster is then reconstructed to produce a 3-d volumetric model, consisting of 2-d image "slices", of the scanned PCB. An X-ray CT slice is a cross-sectional image of a specific region in the 3-d volume that allows to be able to see within the object without cutting. With respect to PCB, the stack of 2-d image slices physically correspond to different locations of depth within the PCB. Although this approach addresses the destructive nature of current RE techniques, there remains a reliance on SMEs to complete the reverse engineering process. Further, RE is compounded by new issues associated with the noise and artifacts in the X-ray data that would not be present in optical images.

Addressing these shortcomings of the current state-of-the-art requires automation., which can be broken down into 5 major areas: image acquisition, image pre-processing, feature extraction, feature analysis, and evaluation. At each stage there are numerous challenges that make automation of RE at the PCB level difficult. Algorithms in pattern recognition, machine learning, and computer vision should be properly adapted to the specific nuances of this application and data set in order to achieve automation.

This paper addresses a challenge seen at the pre-processing stage of the pipeline for PCB RE – automated layer identi-

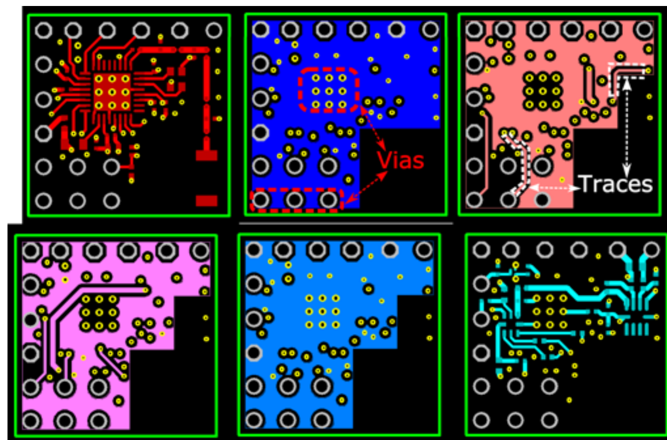

Fig. 1: Digital printed circuit board layout images of RASC PCB. Layers and vias are highlighted with dotted red boxes and white lines.

[1]DISTRIBUTION STATEMENT A. Approved for public release; distribution is unlimited.

fication. The unique aspect of this challenge is the necessity to be unsupervised, or use as little supervision as possible. A naïve approach would be to leverage the current trend of deep learning for classification and identification. While effective, such methods require very large volumes of data to train a classifier in order to learn the general feature distributions of the dataset in hopes of a robust identification network. However, when considering the particular problem space of PCB RE, the quantity of data available is both scarce and quite dynamic. Instead, it is important to identify the properties of the data that generalize across designs in order to be as unsupervised or semi-supervised as possible.

Moreover, it is unknown how much a priori information is available to the user conducting RE. If the user possesses "golden data", or previous design info, it can be used to guide the identification process since the desired outcome is known. However, a holistic identification process needs to be robust enough for varying amounts of golden data. For instance, there could be no prior design information available, such as a legacy electronic system whose original design information has been misplaced through company migrations/attrition. Therefore, it is important that the identification technique proposed be as unsupervised as possible to remove the need for golden data entirely.

This paper, for the first time to the best of our knowledge, addresses all of the above challenges for a generalizable, fully automated, and unsupervised PCB layer identification process. This is achieved by leveraging domain knowledge of the X-ray CT process and PCB design in combination with clustering algorithms to identify what slices belong to what layer in a board in an unsupervised manner. The contributions of this paper are summarized as follows:

1) Fully automated unsupervised 3D-stack alignment via iterative robust regression and registration based on the image gradient direction of the volumetric PCB stack.
2) An optimal framework for fully automated unsupervised X-ray CT slice-to-layer identification of X-ray CT imaged PCBs, which is determined after comparing different combinations of dimensionality reduction algorithms, clustering algorithms, and leveraging the sequential stacking nature of X-Ray CT.
3) Our approach is demonstrated on a 6-Layer PCB that we have designed in house, referred to as RASC, seen in Figure 1.

The remainder of the paper is organized in the following manner: Section II will discuss the experiments in depth, Section III will provide a qualitative and quantitative analysis of the results, and lastly Section IV will conclude the paper.

II. Proposed Methodology

A typical PCB is a multi-layered board where each layer in the board consists of vias (i.e., layer-to-layer interconnects) and traces (i.e., within layer interconnects)[See Figure 1]. Traces are unique to each layer and vias are often in the same location throughout the entire board, except for the case of a blind or buried via unique to a particular layer [4]. Trace patterns are in some instances the most important information since they determine the functionality of the board. Therefore, it is crucial to be able to correctly identify the layers of a PCB during the reverse engineering process. However, this is difficult for a number of reasons.The amount of X-ray CT slices required for 3-d reconstruction varies from sample to sample, and is also a byproduct of parameter optimization during the acquisition process. Further, the actual scanning process requires that the PCB sample in the X-ray chamber be slightly angled in both X and Y to maximize the amount of information acquired during the X-ray process.

Although acquiring the data in this fashion provides a reconstruction of the highest fidelity as far as the acquisition process, relating the X-ray penetration and produced number of slices to a discrete depth in the physical printed circuit board in order to identify the layers is nontrivial. This presents an additional challenge because once reconstructed the data is misaligned causing instances of overlapping/aliased information on slices (i.e., features from a PCB layer below in the stack are present in the layer above or vice versa), as seen in Figure 2, or missing feature information in general. To effectively solve this problem, it is important that the solution not only be able to correctly identify the layer that each slice belongs to but do so in an unsupervised and generalizable manner.

A. Pre-Processing: Alignment

The first challenge that needs to be addressed is the misalignment of slices in a PCB stack. Particularly if the X and Y planes of a PCB stack are not aligned onto the origin of their respective planes it results in missing and/or aliased information of the Z-Axis (top-down) view. With this information missing or distorted, it is near impossible to properly and accurately identify what slices of a stack belong to what particular layer of a PCB. Therefore, the alignment process can be viewed as a necessary pre-processing step.

As mentioned earlier, when a PCB is X-rayed with computed tomography, it results in a 3-dimensional stack of slices. This stack can be reoriented to planar 2-dimensional views in the X, Y, or Z axis. When analyzing the 2-dimensional slices

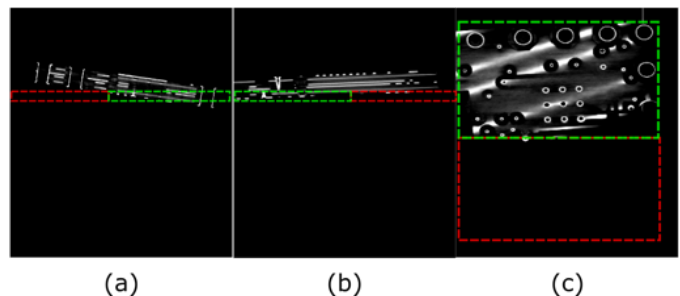

Fig. 2: Raw unaligned X-ray-CT slice in X(a), Y(b), and Z(c). Portions of the slides containing RASC PCB info and those missing information (i.e., aliasing) are highlighted with green and red boxes.

in both the X and Y dimension, it is apparent the displacement from the origin of both axes. Therefore, by simply computing the angle of displacement and rotating the images the board can be better aligned. To achieve this, we employ an iterative realignment process based on robust regressionSpecifically, the centroid of each slice in both the X and Y planes are computed via robust linear regression and the mean displacement from the origin for each slice in each plane is computed. In order to accurately compute the centroids of the images, they are first binarized so a slice represents a distribution of white pixels and their line of best fit represents the centroid of the board. Robust regression with bisquares weighting is used to simply reduce the effect of outlier noise pixels instead of throwing them away altogether since they likely still provide relevant information for the boards alignment. This process is done iteratively and converges once the displacement computed between both planes and the horizontal origin is less than .005 degrees. Figure 3 displays the iterative realignment process on a board designed and X-rayed in our lab, referred to as RASC.

Afterwards, final alignment is refined by computing the image gradient direction of the slices in the stack in the X, Y, and Z direction. The image gradient direction of the slices will provide the directional change in intensity for each direction.By following a heuristic where we can assume that the amount of slices belonging to a layer in the PCB sample will contain at least 6% of the total airless volume we can compute a fused image of the slices that represents the general statistics of the volume with regards to direction. By computing the image gradient on this fused image, the final sample will be optimally registered and aligned. Once this realignment is completed, the stack of slices is ready for slice-to-layer identification.

B. Unsupervised Layer Identification

After alignment, there is now enough information present on each slice such that the physical layers it belongs to on a PCB can be deduced. In order to effectively reverse engineer the design and provide full assurance, it is important that the design can be reproduced in the case where one only has the physical board and X-ray data without prior design knowledge or specifications. This is actually quite common for

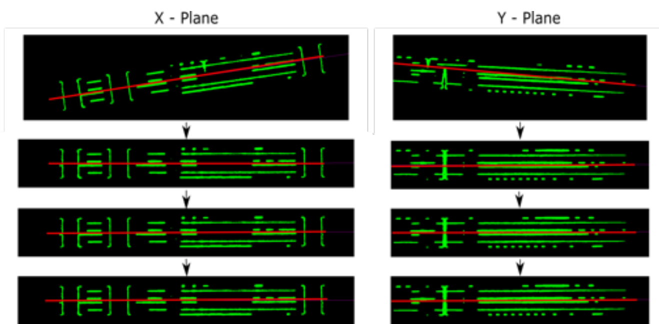

Fig. 3: Iterative regression based realignment with angle of displacement shown in red.

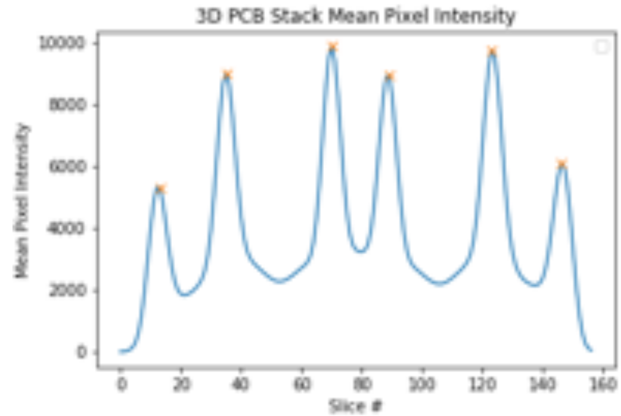

Fig. 4: Mean pixel intensity peaks

legacy electronic systems that have been deployed for years to decades at a time and the design info gets lost or mismanaged [5]. Although there may not be design information available a priori, we can leverage knowledge we have of the X-ray process and board itself.

Specifically, although during the X-ray process one may not have a discrete amount of depth per slice in a stack of images, we do know that they are stacked together sequentially and that each slice is very similar to its neighbors. This means that these slices have a high correlation with one another and lend themselves nicely to clustering algorithms that use correlation as a distance metric. A common algorithm to use for this task is typically K-means , but in order to do this completely unsupervised, one assumes they do not have prior knowledge about the number of layers/clusters a board may contain. This is a major constraint for K-Means. In this paper, we leverage domain knowledge of the X-ray CT process to extract the number of layers in a board stack in an unsupervised manner and use that value as a seed of the K-Means algorithm.

In particular, once a board stack has been optimally aligned its intensities rise and fall as one traverses through it slice by slice in the Z-direction, as seen in Figure 4, peaking where the most information for that respective layer is located. Using this information, a simple peak and valley detection of the mean intensities for each slice of the volume can be used to automatically extract the number of layers. Other data driven approaches to both automatically extract the number of layers in a board and cluster the slices appropriately, such as clustering algorithms DBSCAN or OPTICS [6], [7], are very parameter dependent and difficult to generalize from sample to sample. Furthermore, a deep learning based approach to this problem would face similar generalization challenges due to the lack of labeled data for training and variance across PCB designs.

With the number of layers determined, we can use this value as a seed for K-means clustering with correlation as the distance metric, due to the similarity of slices. In addition to K-means, we analyze using this value as a seed for Gaussian

Mixture Models (GMM), since it is another popular cluster analysis technique whose main hyperparameter is knowing the number of clusters or components a priori.

It is important to note, however, that performing a correlation analysis on these images can become computationally intensive quickly due to the volume of images in a 3-D stack as well as the high resolution of these images in said stack. An additional caveat is that these image slices are very similar to one another (see Figure 5). Therefore, linear dimensionality reduction techniques likely won't suffice since they will either linearly project them in the direction of the most variance which they happen to share, such as Principal Component Analysis (PCA) [8], or require labels to which layer they belong to and are thus supervised like Linear Discriminant Analysis [9]. Instead nonlinear techniques such as Kernel Principal Component Analysis (KPCA) with a radial basis function (RBF) kernel or Multidimensional Scaling (MDS) [10] are applied to project our data to a more discriminant space where the similarities between slices are more pronounced.

In addition to nearby slices having a high correlation to one another, we can leverage the fact that only slices directly near one another will ever belong to the same layer. Therefore, we can apply an exponential windowing function to the correlation feature vectors used for clustering to drastically reduce the impact of slices far away from slices that are under test for classification. The exponential window equation is displayed below,

$$w(X) = e^{\frac{-(i-j)}{\tau}} X_{i,j} \tag{1}$$

where X is the vector of a slice's cross-correlation with respect to every slice in the stack, i is the index of the current slice, and j represents the indices of all the other slices in the stack. The hyperparameter τ is a tunable variable that determines the width of the windowing. Empirically it was determined that the optimal value is to set τ to 6% of the total number of slices present in the stack. Figure 6 displays the cross-correlation of individual slices compared to all other slices in the stack(a) vs. those same slices after exponential windowing(b).

Now with each slice's features more discriminant from dimensionality reduction(PCA, KPCA-RBF, and MDS) and windowing, only those nearest and most similar will cluster to one another after K-means or GMM clustering seeded with the earlier determined number of layers. The final step is to superimpose all slices belonging to their respective layer clusters upon one another to create their respective layer image.

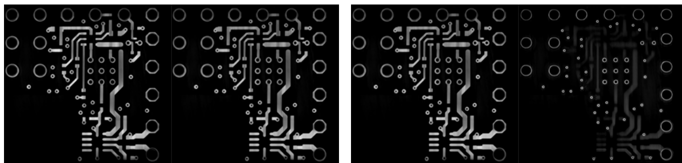

(a) Consecutive PCB Slices (b) Non-Consecutive PCB Slices

Fig. 5: PCB stack slices comparison

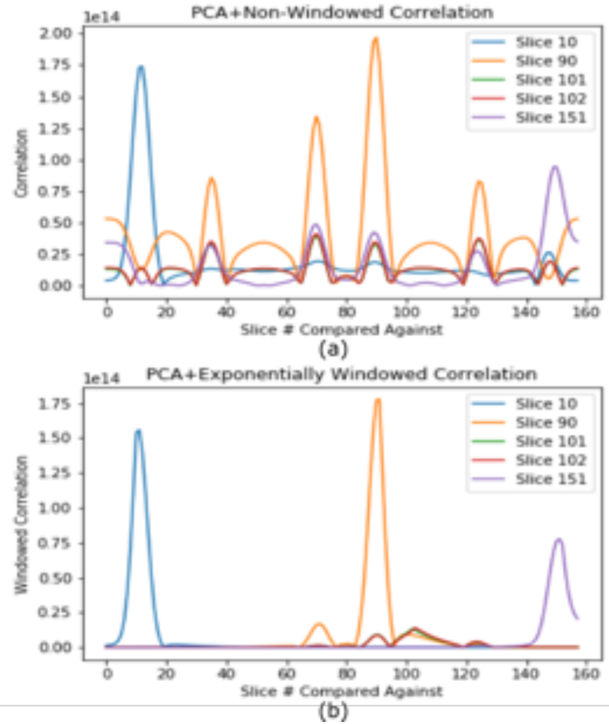

Fig. 6: Cross-correlation comparison: (a) PCA + non-windowed cross-correlation (b) PCA + exponentially windowed cross-correlation

III. Experimental Results and Discussion

The optimal results, and thus final proposed method, for the entire process were achieved via a combination of PCA, exponential windowing, and K-means clustering and can be seen in Figure 7. These can be compared with the known correct PCB layers from the design software in Figure 1. There are currently no established metrics to evaluate the different stages of the RE process or its quality. However, suitable evaluation metrics for this stage are available by leveraging standard classification and clustering metrics. For these metrics the ground truth for comparison are the labels of what slices belong to what specific layers after human evaluation and assignment. Appropriate metrics from a classification perspective are precision, recall, and the resulting F1-Score. These metrics provide an important understanding of false and true positive classifications so false positive classifications don't negatively affect the fusion of a layer's image. From a clustering perspective the appropriate measures are homogeneity, completeness, V-Measure, adjusted mutual information(AMI), and the adjusted rand index(ARI). These measures evaluate, using ground truth labels, how well the different combinations for unsupervised approaches produce clusters where each cluster contains only slices of a single layer (homogeneity) and all slices that belong to a particular layer are assigned to the same layer (completeness).

In Table I, the aforementioned metrics are compared for the unsupervised layer identification framework after utilizing

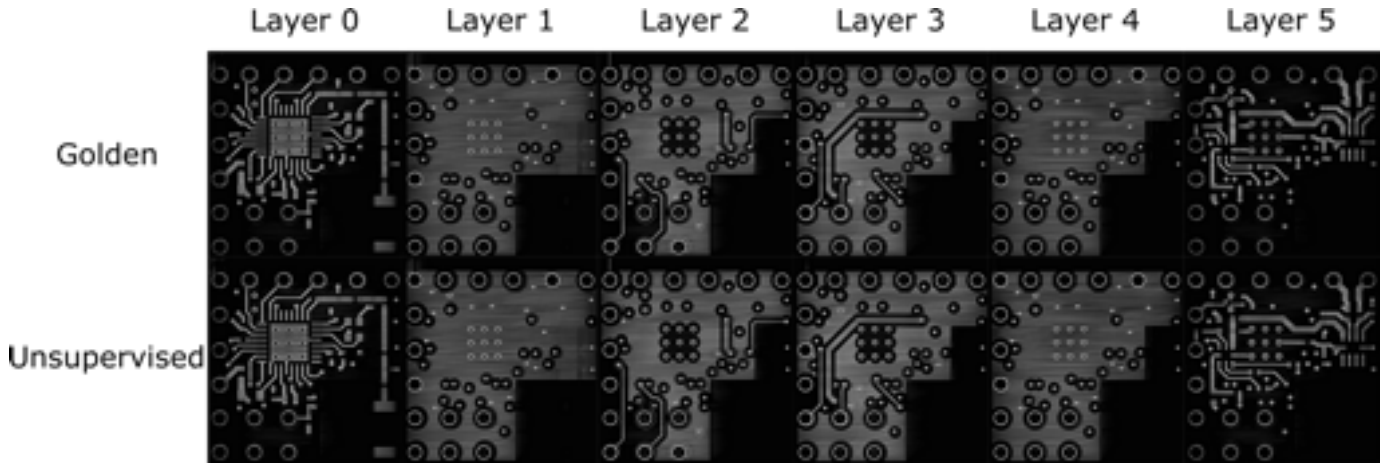

Fig. 7: Unsupervised identification results (PCA + exponentially windowed cross-correlation + K-means clustering) vs. golden images

Average Classification Performance								
Method	Precision	Recall	F1-Score	Homogeneity	Completeness	V-Measure	ARI	AMI
KPCA+Wind. Corr.+K-Means	87.77%	87.77%	87.77%	.821	.816	.818	.738	.806
KPCA+Reg. Corr.+K-Means	1.05%	1.05%	1.05%	.990	.377	.546	.041	.092
MDS+Wind. Corr.+K-Means	56.53%	56.53%	56.53%	.725	.677	.7	.506	.656
MDS+Reg. Corr.+K-Means	5.1%	51%	5.1%	.871	.503	.638	.284	.411
PCA+Reg. Corr.+K-Means	5.1%	5.1%	5.1%	.825	.513	.632	.296	.432
KPCA+Wind. Corr.+GMM	86.91%	86.91%	86.91%	.817	.813	.815	.728	.803
KPCA+Reg. Corr.+GMM	.8%	.8%	.8%	**.996**	.374	.543	.034	.079
MDS+Wind. Corr.+GMM	68.44%	68.44%	68.44%	.832	.778	.804	.691	.763
MDS+Reg. Corr.+GMM	4.78%	4.78%	4.78%	.855	.511	.64	.302	.425
PCA+Wind. Corr.+GMM	86.11%	86.11%	86.11%	.794	.792	.793	.704	.781
PCA+Reg. Corr.+GMM	4.94%	4.94%	4.94%	.836	.5	.626	.285	.407
PCA+Wind. Corr.+K-Means	**90.51%**	**90.51%**	**90.51%**	.828	**.836**	**.832**	**.783**	**.82**

TABLE I: Unsupervised classification performance comparing methods using different combinations of dimensionality reduction algorithms (KPCA Vs. MDS Vs. PCA), correlations (regular cross-correlation vs. exponentially windowed cross-correlation), and clustering algorithms (K-Means Vs. Gaussian mixture models)

Average Image Quality Assessment												
	KPCA+Wind. Corr.+K-Means			PCA+Wind. Corr.+K-Means			KPCA+Wind. Corr.+GMM			PCA+Wind. Corr.+GMM		
Layer	SIR	SSIM	Correlation	SIR	SSIM	Correlation	SIR	SSIM	Correlation	SIR	SSIM	Correlation
0	.823	.892	.9795	.9583	.9053	.9871	.8055	.8767	.9767	.7271	.8547	.9702
1	.9805	.9839	.9948	.9101	.9907	.9985	.9848	.9815	.9938	.9831	.9812	.9957
2	.9799	.989	.9985	.9157	.9916	.9984	.9759	.9822	.9969	.9998	.9872	.9985
3	.9955	.9923	.998	.9283	.9913	.9967	.9871	.9913	.9972	.972	.9902	.9972
4	.9848	.9824	.9931	.9813	.9923	.9993	.9933	.9801	.9912	.9943	.9859	.9983
5	.8715	.9175	.9795	1.0	.9733	.9993	.8591	.9066	.9765	1.0	.9709	.9956

TABLE II: Image quality assessment comparing methods using different combinations of dimensionality reduction algorithms (KPCA Vs. PCA), exponentially windowed cross-correlation, and clustering algorithms (K-means vs. Gaussian mixture models)

a combination of dimensionality reduction techniques (PCA, KPCA-RBF, and MDS), correlation windowing (non-windowed cross-correlation and exponentially windowed cross-correlation), and clustering techniques (K-means and GMM). These results are the average after running our algorithms 100 times for the RASC PCB and the top result for each metric is highlighted in bold. Furthermore, the final proposed method is emphasized at the bottom of Table I, with top scores in all metrics aside from homogeneity. Looking at these results it can be seen that the most important aspect of the identification process is the need for exponential windowing to leverage the location information of each slice with regards to its neighbors. All dimensionality reduction and clustering combinations that did not have exponential windowing did not reach above 10% in terms of classification performance. Furthermore, Table I indicates that the optimal combination for identification in terms of performance is PCA, exponential windowing, and K-means clustering. However, KPCA+Exponential Windowing+K-means, KPCA+Exponential Windowing+GMM, and PCA+Exponential Windowing+GMM were marginally close in terms of performance. Only the combinations with

MDS drastically under-performed and this is likely due to the fact that MDS utilizes the SMACOF (Scaling by MAjorizing a COmplicated Function) algorithm, that utilizes multiple random initializations, similar to K-means, and picks the best one for projecting the data to a lower dimensional space. Optimal performance would come with an increased number of intializations at the cost of drastically increased computation time.

After taking all of these quantitative classification measures into account it is important to remember the main purpose of this stage in the RE process is to produce a high quality image that can be used for later stages in the RE paradigm. Therefore, to measure the level of distortion quantitatively we leverage popular techniques used in the image quality assessment field for reduced reference image comparisons. Specifically, Structural Similarity Index(SSIM), Correlation, and Sift Intensity Ratio (SIR) [11]. SSIM and correlation are metrics that evaluate the pixel level distortion seen between a reference image and test image bounded between 0 and 1. The SIR metric measures the amount of distortion at the feature level. SIR is computed by the following equation

$$r = \begin{cases} \frac{S_d}{S_o} & S_d \leq S_o \\ 1 & S_d > S_o \end{cases}$$

where S_d is the distorted image under test and S_o is the high quality reference image. Taking the ratio between the SIFT points generated from a high-quality reference image compared to the SIFT points generated from a test image the metric is bounded between 0 and 1. A more distorted image should produce less SIFT points than a higher quality image, thus a higher SIR indicates a higher quality image. Taking these metrics into account Table II displays the average image quality assessment results after 100 trials for each layer of the RASC board after unsupervised layer identification for the top 4 combinations from Table I. For the computation of these metrics the images serving as the "Golden" reference images are the fused images derived from human labels for each layer and the "distorted" test images are the fused images of the unsupervised identification framework. Looking at the table, one can see that the scores for each combination were overall very positive and show while there can be some instances of distortion from the ideal layer, it is not drastic.

Furthermore, these results reinforce the classification results that the optimal framework for unsupervised slice-to-layer identification is a combination of leveraging PCA, with exponentially windowed cross-correlation, and K-means clustering. The only metric that the PCA+Exponential Windowing+K-means combination wasn't clearly top compared to the other combinations was SIR. However, it's best to take the combination of all three metrics into account when evaluating instead of just one. When doing so it can be seen that in addition to having improved SIR scores for the surface layers, PCA+Exponential Windowing+K-means has equally high scores in SSIM and Correlation across all layers.

IV. Conclusion

In conclusion, this paper has demonstrated, for the first time, that it is possible to identify what slices of a PCB that has been scanned by X-ray CT belong to what particular layers in the board in an automated and unsupervised fashion. First the crucial pre-processing to align the 3D board stack is achieved in an unsupervised manner that translates across planar board samples. Afterwards, by leveraging domain knowledge of the X-ray CT process and PCB design the number of layers can be extracted and used as a seed for K-Means clustering combined with PCA dimensionality reduction algorithms and exponentially windowed cross-correlation to quickly and accurately determine the correct assortment of slices per PCB layer.

When analyzing the results it can be seen that while there is room for improvement for classification, the image quality isn't drastically affected and thus still produces a usable image for later stages in the automated PCB RE paradigm. This process is especially useful and novel since it can be applied to any PCB that is X-rayed with computed tomography and whether the user has design information a priori or not. Now that this step in the automation process for PCB reverse engineering has been completed, the data is prepared for tackling feature identification and vectorization in future work.

Acknowledgment

This material is based upon work supported by the National Science Foundation Graduate Research Fellowship under Grant No. DGE-1315138 and DGE-1842473.

References

[1] M. o. F. Tehranipoor, U. U. Guin, and S. o. F. Bhunia, "Invasion of the Hardware Snatchers: Cloned Electronics Pollute the Market," *IEEE Spectrum*, 4 2017. [Online]. Available: https://spectrum.ieee.org/computing/hardware/invasion-of-the-hardware-snatchers-cloned-electronics-pollute-the-market

[2] J. Grand, "Printed Circuit Board Deconstruction Techniques," in *Proceedings of the 8th USENIX Workshop on Offensive Technologies - WOOT '14*, 2014. [Online]. Available: https://www.usenix.org/conference/woot14/workshop-program/presentation/grand

[3] N. Asadizanjani, M. Tehranipoor, and D. Forte, "PCB Reverse Engineering Using Nondestructive X-ray Tomography and Advanced Image Processing," *IEEE Transactions on Components, Packaging and Manufacturing Technology*, vol. 7, no. 2, pp. 292–299, 2017.

[4] I. McLoughlin, "Secure embedded systems: The threat of reverse engineering," in *Proceedings of the International Conference on Parallel and Distributed Systems - ICPADS*, 2008, pp. 729–736.

[5] U. J. Botero, M. M. Tehranipoor, and D. Forte, "Upgrade/Downgrade: Efficient and Secure Legacy Electronic System Replacement," *IEEE Design and Test*, vol. 36, no. 1, pp. 14–22, 2019.

[6] E. Schubert, J. Sander, M. Ester, H. P. Kriegel, and X. Xu, "DBSCAN Revisited, Revisited," *ACM Transactions on Database Systems*, vol. 42, no. 3, pp. 1–21, 2017.

[7] M. Ankerst, M. M. Breunig, H.-P. Kriegel, and J. Sander, "Optics," *ACM SIGMOD Record*, vol. 28, no. 2, pp. 49–60, 1999.

[8] J. Shlens, "A Tutorial on Principal Component Analysis," 2014. [Online]. Available: http://arxiv.org/abs/1404.1100

[9] A. J. Izenman, *Modern Multivariate Statistical Techniques*, 2008. [Online]. Available: http://link.springer.com/10.1007/978-0-387-78189-1

[10] I. Borg and P. Groenen, *Modern Multidimensional Scaling - Theory and Applications*. Springer Series in Statistics, 1997.

[11] T. Sun, S. Ding, and W. Chen, "Reduced-reference image quality assessment through SIFT intensity ratio," *International Journal of Machine Learning and Cybernetics*, vol. 5, no. 6, pp. 923–931, 2014.